≪Review Paper≫ Applied Science and Convergence Technology Vol.23 No.5, September 2014, pp.201~210
http://dx.doi.org/10.5757/ASCT.2014.23.5.201

Electronic Structure of the $SrTiO_3$(001) Surfaces: Effects of the Oxygen Vacancy and Hydrogen Adsorption

K. Takeyasu[a], K. Fukada[a], S. Ogura[a], M. Matsumoto[b], and K. Fukutani[a]*

[a]*Institute of Industrial Science, The University of Tokyo, Tokyo 153-8505, Japan*
[b]*Tokyo Gakugei University, Tokyo 184-0015, Japan*

(Received September 24, 2014, Revised September 30, 2014, Accepted September 30, 2014)

The influence of electron irradiation and hydrogen adsorption on the electronic structure of the $SrTiO_3$ (001) surface was investigated by ultraviolet photoemission spectroscopy (UPS). Upon electron irradiation of the surface, UPS revealed an electronic state within the band gap (in-gap state: IGS) with the surface kept at 1×1. This is considered to originate from oxygen vacancies at the topmost surface formed by electron-stimulated desorption of oxygen. Electron irradiation also caused a downward shift of the valence band maximum indicating downward band-bending and formation of a conductive layer on the surface. With oxygen dosage on the electron-irradiated surface, on the other hand, the IGS intensity was decreased along with upward band-bending, which points to disappearance of the conductive layer. The results indicate that electron irradiation and oxygen dosage allow us to control the surface electronic structure between semiconducting (nearly-vacancy free: NVF) and metallic (oxygen de cient: OD) regimes by changing the density of the oxygen vacancy. When the NVF surface was exposed to atomic hydrogen, in-gap states were induced along with downward band bending. The hydrogen saturation coverage was evaluated to be $3.1\pm0.8\times10^{14}$ cm^{-2} with nuclear reaction analysis. From the IGS intensity and H coverage, we argue that H is positively charged as $H^{\sim0.3+}$ on the NVF surface. On the OD surface, on the other hand, the IGS intensity due to oxygen vacancies was found to decrease to half the initial value with molecular hydrogen dosage. H is expected to be negatively charged as H^- on the OD surface by occupying the oxygen vacancy site.

Keywords : Oxygen vacancy, $SrTiO_3$, Hydrogen adsorption

I. Introduction

$SrTiO_3$ is a perovskite-type transition metal oxide with a band gap of about 3.2 eV, and its surface has recently received much attention due to generation of a two-dimensional electron gas [1,2] and photo-catalytic activity under visible light [3,4]. The surfa-ces of oxide materials, however, are readily reduced generating oxygen vacancies, which have substantial influence on the surface electronic structure [5] and play a significant role in the interac-tion with atoms and molecules [6-8]. Characterization of the oxygen

* [E-mail] fukutani@iis.u-tokyo.ac.jp

vacancy, therefore, is indispensable for understanding the functionality of oxide surfaces. The origin of the two-dimensional electron gas on the $SrTiO_3$ surface is indeed claimed to be due to oxygen vacancies [2,9]. Whereas oxygen vacancy formation is usually not a well-controlled pro-cess, it has been shown that oxide surfaces are reduced by irradiation of ultraviolet light and energetic electrons [2,10,11], which might allow us to control the oxygen vacancy concentration.

The interaction of hydrogen with the $SrTiO_3$ surface is of considerable interest and im-portance, because the surface is metalized by hydrogen adsorption [12,13], and molecular hydrogen is formed as a result of photolysis of water [3,4]. It has been shown that the hydrogen adsorbed on the $SrTiO_3$(001) surface forms an O-H bond [13,14]. Since hydrogen is an amphoteric element, hydrogen is possibly adsorbed to cations in addition to anions of oxygen. Such hydrogen-cation complexes, however, have not been identified on the $SrTiO_3$ surface to date. The other possible adsorption site of hydrogen is the oxygen vacancy site. At the oxygen vacancy, hydrogen is expected to form a hydride ion (H^-). It has been suggested that a vacancy-hydrogen complex is formed with hydrogen negatively charged in $SrTiO_3$ bulk experimentally [15,16] and theoretically [17]. Previous photoemission studies have shown that the in-gap state generated by ion bombardment or annealing on a $SrTiO_3$(111) is decreased by H_2 dosage [18,19]. Although the studies suggest hydrogen interaction with oxygen vacancies, these studies were conducted on a disordered surface, and the detailed investigation remained to be done. The motivation behind the present study is thus to prepare an oxygen-deficient surface in a controlled manner and to clarify the interaction of hydrogen and concomitant charge transfer with the $SrTiO_3$ surfaces with and without oxygen vacancies.

In the present article, we review our recent work on the electronic structure of the $SrTiO_3$(001) surface investigated by ultraviolet photoemission spectroscopy (UPS) [20,21]. We first show that an in-gap state (IGS) appears within the band gap with electron irradi-ation, which is caused by oxygen vacancies. We also show that electron irradiation causes a band bending inducing an insulator to metal transition in the surface layer. We then demonstrate that the effects of hydrogen on the electronic structure of the $SrTiO_3$(001) surface with and without oxygen vacancies. On a nearly-vacancy-free (NVF) surface, hydrogen atoms are adsorbed with an atomic-hydrogen dose revealing an in-gap state. The hydrogen coverage is quantitatively analyzed to be $3.1\pm0.8\times10^{14}$ cm^{-2} with nuclear reaction analy-sis (NRA). Upon molecular hydrogen exposure to an oxygen-deficient (OD) surface, on the other hand, the in-gap state due to oxygen vacancies decreases in intensity in contrast to the NVF surface. We discuss that the adsorbed hydrogen is positively charged on the NVF surface and negatively charged on the OD surface.

II. Experimental

The $SrTiO_3$(001) surface was cleaned by annealing at 923 K under 6.5×10^{-4} Pa of oxygen gas for 30 min, which is expected to lead to dominant termination by the TiO_2 layer with a slight mixture of the SrO layer [22]. The surface was then annealed in ultrahigh vacuum (UHV) at 1000 K for 10 min. This process introduces oxygen vacancies in the bulk without causing any reconstructions at the surface, which brings about electric conductivity allowing UPS measurements without charging-up. The density of the oxygen vacancy on the surface induced by annealing is $\langle\langle10^{13}$ cm^{-2}, which we regard as an NVF surface [20]. The NVF surface was reduced by irradiation of electrons with an energy of 1500 eV at a sample temperature of room temperature.

The interaction of hydrogen with the $SrTiO_3$(001)

surface was examined by introducing H_2 gas (99.999 % purity) into the UHV chamber after purification with a palladium mem-brane heated at 400°C. Atomic hydrogen was produced by passing the purified H_2 gas in a tungsten tube heated at 1900 K. In the present experiments, the $SrTiO_3$(001) surface was exposed to either molecular H_2 or atomic H at room temperature.

The surface electronic structure was investigated by using UPS with the He I line (21.22 eV) at an incident angle of 45° in normal emission at room temperature. The absolute amount of hydrogen and its depth profile were investigated by the $^{1}H(^{15}N, \alpha\gamma)^{12}C$ nuclear reaction at the 1E beamline of the 5 MV Van de Graaff Tandem accelerator in the Mi-croanalysis Laboratory (MALT) of The University of Tokyo [23,24]. The $^{15}N^{2+}$ ion beam irradiated the surface at a current of 40~100 nA and a beam diameter of 2~4 mm on the surface at room temperature. By detecting the γ-ray at 4.43 MeV emitted in the nuclear reaction, the absolute H concentration was evaluated by calibrating the γ-detection effciency of the system with a kapton film with a known H concentration. Since the nuclear reaction is resonanced at 6.385 MeV with a resonance width of 1.8 keV, the hydrogen depth distribution was analyzed by using the stopping power (2.67 keV/nm for $SrTiO_3$) [25]. The depth resolution is a few nanometers mainly due to the Doppler-broadening of the resonance peak [26].

III. Results and Discussion

1. Oxygen vacancy formation

Fig. 1(a) shows the UPS spectrum for the NVF $SrTiO_3$ (001) surface. The large intensity below −3.1 eV corresponds to the valence band mainly due to O 2*p* of $SrTiO_3$. The inset shows the spectrum near the Fermi level (E_F). No particular feature was observed between E_F and −3.1 eV except background and a

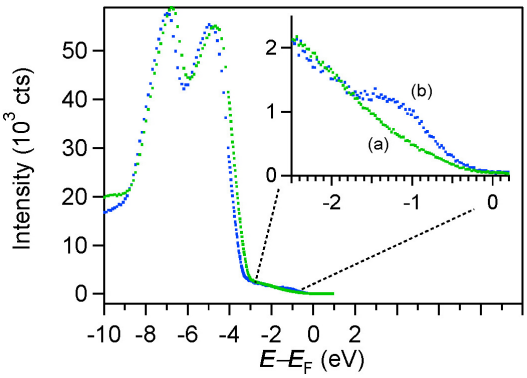

Figure 1. UPS spectra of (a) NVF (green) and (b) electron-irradiated (blue) $SrTiO_3$(001) surfaces with a photon energy of 21.2 eV taken at room temperature. The inset shows the spectra near E_F. The electron irradiation was performed at an energy of 1500 eV and the electron dose was 5×10^{18} cm^{-2}. Adapted with permission from [20].

hump at −2.7 eV, which was ascribed to the emission due to the 23.1 eV line of He I [27]. The position of the valence band maximum (E_V) was evaluated to be −3.1 eV by linear extrapolation of the valence band to the zero intensity. After electron irradiation of 5.0×10^{18} cm^{-2}, the spectrum revealed an electronic state in the band gap at 1.3 eV below E_F, as shown in Fig. 1(b). This in-gap state (IGS) is likely to be induced by electron doping into the Ti 3*d* band of $SrTiO_3$ [12,28,29]. Along with the appearance of the IGS, E_V was shifted toward a lower energy. Electron irradiation causes electronic excitation at the surface, which often induces desorption of adsorbates or substrate atoms. A likely species is oxygen in the substrate of $SrTiO_3$, which generates oxygen vacancies in the substrate. The IGS is therefore considered to be caused by oxygen vacancies on the topmost surface, as schematically shown in Fig. 2(a) and (b). An oxygen atom is expected to desorb as a neutral species, which was originally O^{2-} in $SrTiO_3$ (001). As a result, the two electrons in O^{2-} are transferred to the Ti 3*d* band on the surface, and the doped electrons are spatially localized forming IGS. The mechanism of the electron localization has been discussed in terms

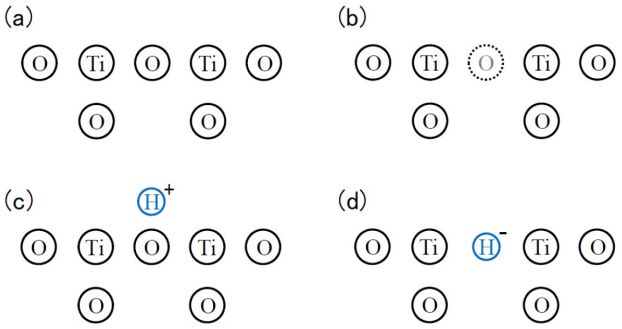

Figure 2. Schematic gures of the surface structure. (a) Vacancy-free surface, (b) oxygen-de cient surface, (c) H-adsorbed at the O site, and (d) H at the oxygen vacancy site.

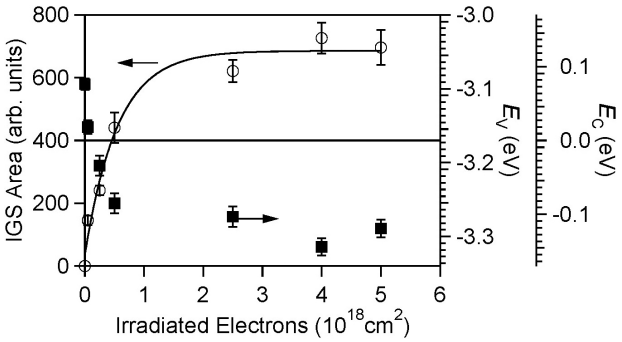

Figure 3. Peak area of the in-gap state, and positions of the valence band maximum and conduction band minimum on the NVF $SrTiO_3$ (001) surface as a function of the electron dose with an electron energy of 1500 eV. Reproduced with permission from [20].

of the polaronic effect [30] and the Ti 3*d*-O 2*p* hybridization effect [31]. Note that LEED after electron irradiation revealed only 1×1 with a slight increase of the background intensity indicating that the oxygen vacancy was randomly distributed on the surface.

Fig. 3 shows the peak area of IGS and the position of E_V as a function of the number of irradiated electrons on the NVF surface. The position of the conduction band minimum (E_C) was evaluated by adding the bulk band gap energy of 3.17 eV to E_V [32,33], which is also shown in the figure. The peak area of IGS increases with increasing electron dose and saturates at about 2×10^{18} cm^{-2}. The oxygen desorption

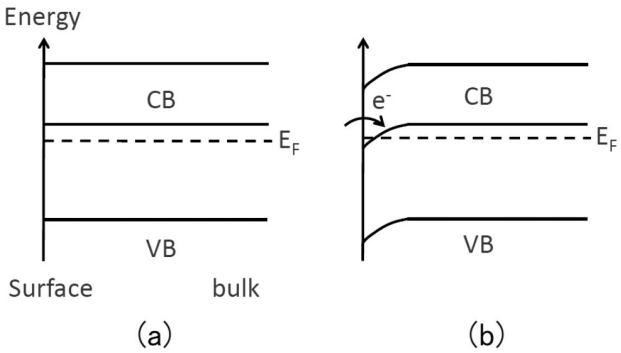

Figure 4. Schematic illustrations of the energy band from the surface to bulk. (a) Nearly at band corresponding to the NVF surface. (b) Band downward-bent at the surface corresponding to the OD and H-adsorbed NVF surfaces.

cross section is estimated to be 1.8×10^{-18} cm^2 from a fit with an exponential function. This value is smaller than that for TiO_2 of 9×10^{-17} cm^2 [10], probably because oxygen atoms are more strongly bound in $SrTiO_3$ than in TiO_2 [34]. Fig. 3 also shows that the electron irradiation lowers E_V from −3.09 eV to −3.29 eV and E_C from 0.08 eV to −0.12 eV. This means that there occurred a downward band bending near the surface as schematically shown in Fig. 4. Electrons are transferred to the substrate and E_C seems to cross E_F suggesting formation of a conductive layer on the surface. Nevertheless, metallic states at E_F were not observed with electron irradiation of 5×10^{-18} cm^{-2} as shown in Fig. 1(a). This is probably because the photon energy of the He I line is not sensitive to the metallic state [29,31]. It is noted that presence of IGS and a metallic state in the conduction band with an oxygen vacancy is consistent with recent theoretical calculations that the in-gap state due to an oxygen vacancy is singly occupied by a doped electron with the other electron in the conduction band [35]. We also note that E_C seems to cross E_F at a certain electron dose while IGS starts to grow from zero dose. This suggests that the IGS is not caused by a side effect of the metallic state in the photoemission process.

When the electron-irradiated surface was exposed

to molecular oxygen, the IGS was found to decrease in intensity and eventually disappear at an oxygen exposure of ~2.5 L. This is because neutral oxygen is either dissociatively or molecularly adsorbed at the oxygen vacancy receiving electrons from the surface. At the same time, E_V and E_C shift toward a higher energy, and E_C crosses E_F quenching the conductive layer on the surface. As a result, the surface is considered to be depleted. On the assumption that the oxygen adsorption at the oxygen vacancy site is a first-order reaction with a sticking probability of 0.6 [36], the density of the oxygen vacancy produced by electron irradiation was estimated to be 1×10^{14} cm^{-2} from the reduction rate of the IGS intensity.

2. Hydrogen on nearly-vacancy free surface

Fig. 5 shows the UPS spectra near E_F for the NVF surface before and after an atomic-H exposure of 9×10^3 L (1 L = 1.33×10^{-4} Pa · s). Whereas the spectrum reveals no change with H_2 exposure to the NVF surface, the intensity in the band gap region is significantly enhanced by atomic H exposure. This is also an in-gap state as observed on the OD surface produced by electron irradiation. The peak area of IGS and E_V as a function of the atomic-H exposure are shown in Fig. 6. The peak area increased with increasing H exposure and saturated at about 3×10^3 L. The peak area at saturation was 44% of that of the OD surface. At the same time, E_V was lowered from −3.12 eV to −3.17 eV, and the work function changed by −0.3 eV. With the H exposure, furthermore, a small feature developed at −10.5 eV, which is attributed to the O-H bond implying that hydrogen is adsorbed on the oxygen atom as schematically shown in Fig. 2(c) [13,37]. These results indicate electron transfer from hydrogen to the surface. The decrease of the work function is considered to be caused by the electric dipole moment at the O-H bond. Note that E_C is estimated to change from 0.05 to 0 eV from the change of E_V on the assumption of the band gap of 3.17 eV. It is also noted that a metallic state was not observed in the UPS spectrum of Fig. 5(b) although E_C is expected to lie near E_F. This is because of the photon energy of 21.22 eV used in the present study. The metallic state appears around the Γ point, which can be effciently excited to a final state at 81 eV above E_F with a photon en-

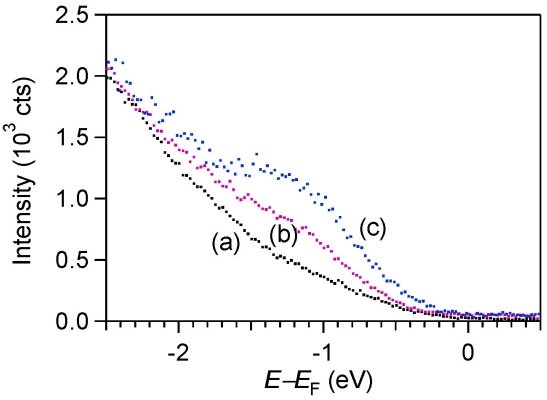

Figure 5. UPS spectra taken at room temperature for (a) the NVF $SrTiO_3$(001) surface (black), (b) the NVF surface exposed to atomic H of 9×10^3 L (red) and (c) the OD surface (blue) at a photon energy of 21.22 eV near E_F. Adapted with permission from [21].

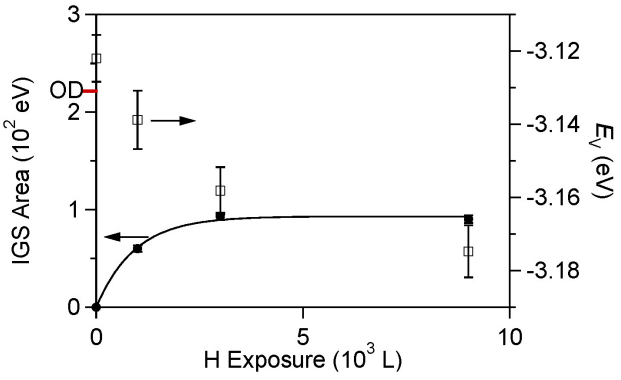

Figure 6. Peak area of the in-gap state and the position of the valence band maximum (E_V) in Fig. 5 as a function of the atomic H exposure on the NVF $SrTiO_3$(001) surface. The mark on the ordinate indicated by OD denotes the IGS area for the OD surface. Adapted with permission from [21].

ergy of 81 eV [12].

The NRA yield curves measured for the NVF surface before and after atomic-H dosage of 5×10^4 L are shown in Fig. 7(a) and (b). The profiles reveal a maximum at the resonance energy indicating that H is present at the surface within the experimental uncertainty. For the NVF surface, the H coverage is estimated to be $(2.2\pm0.4)\times10^{14}$ cm^{-2} even without hydrogen exposure. The observed signal might originate from hydrogen trapped at defect sites due to background gas adsorption, although the origin remains to be elucidated. The profile after atomic-H dosage, on the other hand, shows an enhanced intensity at the resonance energy, indicating that hydrogen is adsorbed on the surface. The amount of hydrogen adsorbed on the surface is estimated to be $(3.1\pm0.8)\times10^{14}$ cm^{-2} by subtracting the H coverage value observed for the NVF surface from that obtained after atomic H exposure. This corresponds to 0.47 hydrogen in the surface unit cell of TiO_2.

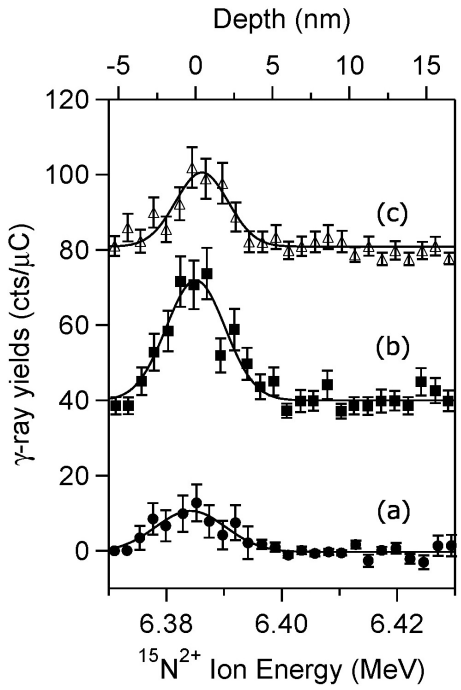

Figure 7. Yield curves of the $^1H(^{15}N, \alpha\gamma)^{12}C$ nuclear reaction taken at room temperature for (a) the NVF $SrTiO_3$(001) surface, (b) the NVF surface exposed to atomic H, and (c) the oxygen-deficient $SrTiO_3$(001) surface exposed to H_2. Adapted with permission from [21].

The charge transfer and charged state of H can be discussed on the basis of the above experimental results. It is noted that atomic hydrogen might abstract the oxygen atom on the NVF surface as a water molecule, which leads to formation of the oxygen vacancy on the surface exhibiting IGS as shown in Fig. 1. However, oxygen abstraction by atomic hydrogen is unlikely to occur on $SrTiO_3$, because oxygen atoms are more strongly bound in $SrTiO_3$ than TiO_2 and oxygen abstraction on TiO_2 is induced only above 500 K [38-40]. The IGS observed in Fig. 5 is, therefore, induced by hydrogen adsorbed on oxygen at the surface.

The area density of electrons donated from H to the surface is evaluated from the IGS intensity observed in UPS. As discussed in Sec. III.A, the IGS intensity on the OD surface shown in Fig. 1 corresponds to the surface electron with an area density of 2×10^{14} cm^{-2} (twice as many as the oxygen vacancy density). On the assumption that the IGS intensity is proportional to the surface electron density in IGS, the areal electron density on the H-adsorbed NVF surface is estimated to be 0.8×10^{14} cm^{-2}. This value is similar to the electron density of 0.6×10^{14} cm^{-2} estimated from the Fermi wavevector of the metallic state in previous work [12]. Since the hydrogen coverage on this surface is 3.1×10^{14} cm^{-2}, a hydrogen atom is considered to donate ~0.3 electron to the surface as $H^{0.3+}$. This electron transfer leads to formation of a dipole layer on the surface. We assume that the O-H bond length is 0.1 nm, the permittivity changes from the vacuum value of ε_0 to that of $SrTiO_3$ (~$300\varepsilon_0$ [41]) at the middle of the O-H, and the charge of hydrogen uniformly distributes from the top to the half of the O-H bond. Then, the potential difference in this layer is evaluated to be 0.4 V, which is in rough agreement with the workfunction change of 0.3 eV.

3. Hydrogen on oxygen-de cient surface

For the NVF surface, UPS revealed no change upon molecular H_2 dosage. On the OD surface, on the other hand, a significant effect was observed in UPS. Fig. 8 shows the change in the UPS spectrum near E_F by H_2 exposure on the OD surface. For the OD surface, IGS is present at −1.3 eV in the band gap, which is caused by oxygen vacancies on the topmost surface as discussed in Sec. III.A. After a H_2 exposure of 2.5×10^4 L on the OD surface, the peak area of the IGS was found to decrease as shown in Fig. 8. The peak area of the IGS and E_V as a function of H_2 exposure are shown in Fig. 9. The peak area of the IGS was reduced by H_2 exposure to a half of the initial value. It appears that the electrons in the IGS induced by oxygen vacancies were withdrawn by adsorbed hydrogen. Furthermore, the work function was reduced by 0.1 eV, and E_V was shifted from −3.22 eV to −3.16 eV. This indicates that the band is upward bent and that E_C crosses E_F suppressing the conductive layer originating from the surface oxygen vacancy.

Fig. 7(c) shows the NRA yield curve taken after a H_2 dosage of 1×10^5 L on the OD surface. With the H_2 dosage, the NRA intensity is slightly increased as compared with the result of Fig. 7(a). The hydrogen coverage due to the H_2 dosage is estimated to be $(0.9\pm0.7)\times10^{14}$ cm^{-2}. Although the uncertainty is large, this value is similar to the oxygen vacancy density of 1×10^{14} cm^{-2} induced by electron irradiation suggesting that a hydrogen atom adsorbs at the oxygen vacancy site. This appears to indicate that one hydrogen receives one electron from the OD surface and the hydrogen exists in the H^- state, which is in remarkable contrast with the adsorption state of hydrogen on the NVF surface in which H is positively charged.

Previous experimental studies claimed that H^- is present at the oxygen site in bulk oxides [42-45]. It is also theoretically shown that oxygen vacancies are stably occupied by hydrogen as H^- in TiO_2, $BaTiO_3$ and $SrTiO_3$ [17,48,49]. We discuss in the following the stability of H^- around the oxygen vacancy on the $SrTiO_3$(001) surface. The total energy is approximately evaluated by taking account of the electronic energy for H^- formation and the electrostatic potential of H^- in the ionic lattice, because H^- is a closed-shell ion. The energy required for the H^- formation on $SrTiO_3$ is evaluated by

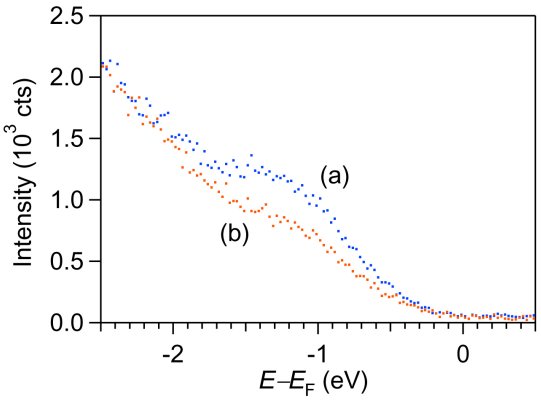

Figure 8. (a) UPS taken at room temperature for (a) the OD $SrTiO_3$(001) surface (blue) and (b) the OD surface exposed to H_2 of 2.5×10^4 L (red) with a photon energy of 21.22 eV. Adapted with permission from [21].

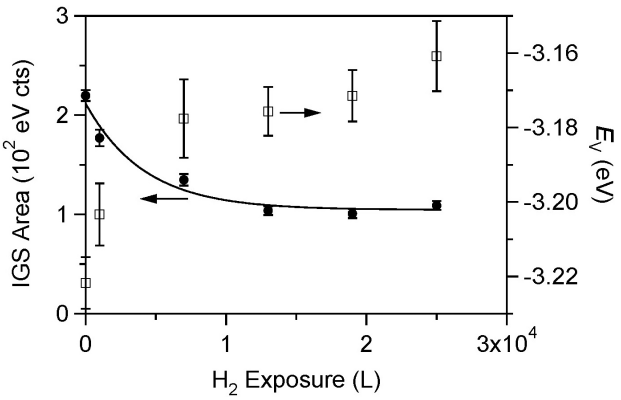

Figure 9. Peak area of the in-gap state and the position of the valence band maximum (E_V) on the OD surface in Fig. 8 as a function of the H_2 exposure. Adapted with permission from [21].

$$SrTiO_3 + \frac{1}{2}H_2 \rightarrow SrTiO_3^+ + H^-$$

The dissociation energy of H_2 and the electron affnity of H are 2.3 eV/H [50] and 0.8 eV [50], respectively. The ionization energy of $SrTiO_3$ is assumed to be the sum of the work function (5.1 eV) [51] and the energy of the IGS from E_F (1.3 eV). As a result, the energy required for the above reaction becomes 7.9 eV. The energy gain due to adsorption of H^- on $SrTiO_3^+$ mainly originates from the electrostatic potential energy between H^- and the ions in $SrTiO_3^+$. The electrostatic potential energy is calculated from the Madelung energy and the repulsive energy between the electron orbital of H^- and $SrTiO_3$(001)+ with a surface oxygen vacancy. The Madelung energy was calculated as a function of the H^- position with the Ewald method [52], which represents a local maximum of 19.5 eV at the oxygen vacancy site along the [100] direction. This is because of the attractive interaction from the neighboring Ti ions. Along the [010] and [001] directions, on the other hand, the Madelung energy shows a minimum at the oxygen vacancy site. The repulsive energy U is assumed to be the Born-Mayer type function given by $U = a\exp(-d/b)$, where d is the distance between the centers of ions and a and b are the Born-Mayer parameters for each pair of ions. The Born-Mayer parameters are adjusted with the measured H^- radii [21, 53]. Although the actual H^- radius is not known, the total energy takes positive values on Ti and O atoms, and reveals a negative value only around the oxygen vacancy site. This indicates that H^- can stably adsorb only at the oxygen vacancy site on $SrTiO_3$(001) due to the large gain of the electrostatic potential energy.

IV. Conclusion

We have reviewed our recent work on the electronic structure of the $SrTiO_3$(001) surface. By applying electron irradiation, oxygen vacancies were formed on the surface, which revealed an in-gap state and downward band bending. By tuning the electron dose and oxygen exposure, the surface was switched between the metallic and insulating regimes. Whereas H adsorption induced an in-gap state on the nearly-vacancy-free $SrTiO_3$(001) surface, the in-gap state due to oxygen vacancies was partially removed by H on the oxygen-deficient $SrTiO_3$(001) surface. By taking account of the absolute H coverage and the in-gap state intensity, we argued that hydrogen is positively and negatively charged on the nearly-vacancy-free and oxygen-deficient surfaces, respectively.

Acknowledgements

This work was supported by Grant-in-Aid for Scientific Research (Grant numbers 11J09249, 24246013 and 24108503) of Japan Society for the Promotion of Science (JSPS).

References

[1] A. F. Santander-Syro, O. Copie, T. Kondo, F. Fortuna, S. Pailhes, R. Weht, X. G. Qiu, F. Bertran, A. Nicolaou, A. Taleb-Ibrahimi, P. Le Fevre, G. Herrantz, M. Bibes, N. Reyren, Y. Apertet, P. Lecoeur, A. Barthelemy, and M. J. Rozenberg, Nature **469,** 189 (2011).

[2] W. Meevasana, P. D. C. King, R. H. He, S.-K. Mo, M. Hashimoto, A. Tamai, P. Songsiririt-thigul, F. Baumberger, and Z.-X. Shen, Nat. Mater. **10,** 114

(2011).

[3] A. Kudo and Y. Miseki, Chem. Soc. Rev. **38,** 253 (2009).

[4] Y. Kuo and K. J. Klabunde, Nanotechnology **23,** 294001 (2012).

[5] D. A. Muller, N. Nakagawa, A. Ohtomo, J. L. Grazul, and H. Y. Hwang, Nature **430,** 657 (2004).

[6] V. E. Henrich, Prog. Surf. Sci. **9,** 143 (1979).

[7] S. Azad, M. H. Engelhard, and L.-Q. Wang, J. Phys. Chem. B **109,** 10327 (2005).

[8] J. Baniecki, M. Ishii, K. Kurihara, K. Yamanaka, T. Yano, K. Shinozaki, T. Imada, K. Nozaki, and N. Kin, Phys. Rev. B **78,** 195415 (2008).

[9] J. Shen, H. Lee, R. Valent, and H. O. Jeschke, Phys. Rev. B **86,** 195119 (2012).

[10] O. Dulub, M. Batzill, S. Solovev, E. Loginova, A. Alchagirov, T. E. Madey, and U. Diebold, Science **317,** 1052 (2007).

[11] C. M. Yim, C. L. Pang and G. Thornton, Phys. Rev. Lett. **104,** 036806 (2010).

[12] M. D'Angelo, R. Yukawa, K. Ozawa, S. Yamamoto, T. Hirahara, S. Hasegawa, M. Silly, F. Sirotti, and I. Matsuda, Phys. Rev. Lett. **108,** 116802 (2012).

[13] R. Yukawa, S. Yamamoto, K. Ozawa, M. D'Angelo, M. G. Silly, F. Sirotti, and I. Matsuda, Phys. Rev. B **87,** 115314 (2013).

[14] F. Lin, S. Wang, F. Zheng, G. Zhou, J. Wu, B. L. Gu, and W. Duan, Phys. Rev. B **79,** 35311 (2009).

[15] B. Jalan, R. Engel-Herbert, T. E. Mates, and S. Stemmer, Appl. Phys. Lett. **93,** 52907 (2008).

[16] J.-H. Ahn, P. C. McIntyre, L. W. Mirkarimi, S. R. Gilbert, J. Amano, and M. Schulberg, Appl. Phys. Lett. **77,** 1378 (2000).

[17] Y. Iwazaki, Y. Gohda, and S. Tsuneyuki, APL Materials **2,** 012103 (2014).

[18] S. Ferrer and G. A. Somorjai, Surf. Sci. **94,** 41 (1980).

[19] F. T. Wagner, S. Ferrer, and G. A. Somorjai, Surf. Sci. **101,** 462 (1980).

[20] K. Takeyasu, K. Fukada, M. Matsumoto, and K. Fukutani, J. Phys.: Condens. Matter **25,** 162202 (2013).

[21] K. Takeyasu, K. Fukada, S. Ogura, M. Matsumoto, and K. Fukutani, J. Chem. Phys. **140,** 084703 (2014).

[22] Y. Liang and D. A. Bonnell, Surf. Sci. **310,** 128 (1994).

[23] K. Fukutani, Curr. Opin. Solid State Mater. Sci. **6,** 153 (2002).

[24] M. Wilde and K. Fukutani, Surf. Sci. Rep. in press.

[25] J. F. Zieqler, Handbook of stopping cross-sections for energetic ions in all elements (Pergamon Press, New York, 1980).

[26] K. Fukutani, A. Itoh, M. Wilde, and M. Matsumoto, Phys. Rev. Lett. **88,** 116101 (2002).

[27] V. E. Henrich, G. Dresselhaus, and H. J. Zeiger, Phys. Rev. B **17,** 4908 (1978).

[28] V. E. Henrich, G. Dresselhaus, and H. J. Zeiger, Solid Stat. Commun. **24,** 623 (1977).

[29] A. Fujimori, I. Hase, M. Nakamura, H. Namatame, Y. Fujishima, Y. Tokura, M. Abbate, F. M. F. de Groot, M. T. Czyzyk, and J. C. Fuggle, Phys. Rev. B **46,** 9841 (1992).

[30] J. L. M. van Mechelen, D. van der Marel, C. Grimaldi, A. B. Kuzmenko, N. P. Armitage, N. Reyren, H. Hagemann, and I. I. Mazin, Phys. Rev. Lett. **100,** 226403 (2008).

[31] Y. Ishida, R. Eguchi, M. Matsunami, K. Horiba, M. Taguchi, and A. Chainani, Phys. Rev. Lett. **100,** 56401 (2008).

[32] R. Moos and K. H. Härdtl, J. Am. Ceram. Soc. **80,** 2549 (1997).

[33] A. Rothschild, W. Menesklou, H. L. Tuller, and I.-T. Ellen, Chem. Mater. **18,** 3651 (2006).

[34] Q. Fu and T. Wagner, J. Phys. Chem. B **109,** 11697 (2005).

[35] Z. Hou and K. Terakura, J. Phys. Soc. Jpn. **79,** 114704 (2010).

[36] M. A. Henderson, W. S. Epling, C. L. Perkins, C. H. F. Peden, and U. Diebold, J. Phys. Chem. B **103,** 5328 (1999).

[37] P. A. Thiel and T. E. Madey, Surf. Sci. Rep. **7,** 211 (1990).

[38] J. Tao, Q. Cuan, X.-Q. Gong, and M. Batzill, J. Phys. Chem. C **116,** 20438 (2012).

[39] E. Cho, S. Han, H.-S. Ahn, K.-R. Lee, S. Kim, and C. Hwang, Phys. Rev. B **73,** 193202 (2006).

[40] R. Astala and P. D. Bristowe, Modelling Simul. Mater. Sci. Eng. **9,** 415 (2001).

[41] R. C. Neville, B. Hoeneisen, and C. A. Mead, J. Appl. Phys. **43,** 2124 (1972).

[42] Y. Chen, M. M. Abraham, L. C. Templeton, and W. P. Unruh, Phys. Rev. B **11,** 881 (1975).

[43] Y. Chen, V. M. Orera, R. Gonzalez, R. T. Williams, G. P. Williams, G. H. Rosenblatt, and G. J. Pogatshnik, Phys. Rev. B **42,** 1410 (1990).

[44] K. Hayashi, S. Matsuishi, T. Kamiya, M. Hirano, and H. Hosono, Nature **419,** 462 (2002).

[45] Y. Kobayashi, O. J. Hernandez, T. Sakaguchi, T. Yajima, T. Roisnel, Y. Tsujimoto, M. Morita, Y. Noda, Y. Mogami, A. Kitada, M. Ohkura, S. Hosokawa, Z. Li, K. Hayashi, Y. Kusano, J. E. Kim, N. Tsuji, A. Fujiwara, Y. Matsushita, K. Yoshimura, K. Takegoshi, M. Inoue, M. Takano, and H. Kageyama, Nat. Mater. **11,** 507 (2012).

[46] F. Filippone, G. Mattioli, P. Alippi, and A. A. Bonapasta, Phys. Rev. B **80,** 245203 (2009).

[47] Y. Iwazaki, T. Suzuki, and S. Tsuneyuki, J. Appl. Phys. **108,** 83705 (2010).

[48] D. R. Lide, CRC handbook of chemistry and physics (CRC Press, Boca Raton London New York Washington, D.C., 2001), 82nd ed.

[49] F. Lenzmann, J. Krueger, S. Burnside, K. Brooks, M. Gra, D. Gal, S. Ru, and D. Cahen, J. Phys. Chem. B **105,** 6347 (2001).

[50] P. P. Ewald, Ann. Phys. **64,** 253 (1921).

[51] G. G. Libowitz and T. R. P. Gibb Jr., J. Phys. Chem. **60,** 510 (1956).